

room temperature appeared to become faster at low temperatures. This apparent fast quenching may be ascribed to the MV^{2+} frozen out at the originally solubilized sites close to pyrene in the micelle. However, at room temperature, increased mobility of the solutes may tend to separate them from each other within the lifetime of pyrene in the excited state. This gives rise to a slower quenching reaction at room temperature. The pronounced immediate intensity reduction at a low temperature may be explained by the increase in the association constant with decreasing temperature. In the $C_{16}C_2V^{2+}$ quenching system, the similarity of the time-dependent quenching at room temperature and at 77 K may be explainable by the assumption that reaction is possible for $C_{16}C_2V^{2+}$ without attaining close contact with excited pyrene. Diffusional motion at room temperature may serve only to average the reactants separation. Both CP^+ and MV^{2+} (or $C_{16}C_2V^{2+}$) are known to be good electron acceptors, and the viologen ion has a stronger electron affinity than the pyridinium ion. Accordingly, the above results strongly suggest the occurrence of an electron-tunneling process, i.e., long-range electron transfer in the $C_{16}C_2V^{2+}$ system, although electron transfer is basically the mechanism also for CP^+ quenching. The strong dependence of the electron-transfer rate from the excited pyrene to viologen ion on the separation of quencher-quencher pair supports this hypothesis.

Other quenchers for pyrene investigated in this study were Cu^{2+} , Eu^{3+} , Ag^+ , Tl^+ , N,N' -dimethylaniline (DMA), nitrobenzene (NB), and CCl_4 . With metal ions, the effect of quencher on the time-dependent pyrene fluorescence decay is not appreciable at concentrations of less than several millimolar. This may be partly due to the decreased permeability of the micelle in an EGW solution compared to that of a normal NaLS micelle. The data emphasize the necessity of diffusional motion of metal ions for the quenching of singlet pyrene in micellar systems. However, at more than 10 mM, Cu^{2+} exhibited $C_{16}C_2V^{2+}$ -type quenching, and both Ag^+ and Tl^+ exhibited MV^{2+} -type quenching. Pyrene phosphorescence was detected in the latter system,²⁸ and

ground-state complexation was also detected in absorption-spectra studies. The quenching by DMA was classified into the CP^+ type although that by NB and by CCl_4 were of the $C_{16}C_2V^{2+}$ type. These quenchers are supposed to reside inside the micelle. The decreased quenching ability of DMA at 77 K may imply an importance of orientational factors for electron transfer in this system as well as the necessity of motion, since the separation of pyrene and DMA is expected to be small in these studies.

In conclusion, electron tunneling, i.e., long-range electron transfer, does not seem to be a predominant mechanism as far as common luminescence-quenching reactions in a micellar system at room temperature are concerned. Inhibition of motion by freezing in order to observe long-range phenomena is critical. The short lifetime of excited species also seems to contribute to the difficulty of instituting efficient tunneling processes. However, it is likely that more efficient tunneling becomes operative in certain triplet quenching reactions because of the longer lifetime of these excited states. The frozen micellar systems demonstrated here offer some advantages for studies to gain a better understanding of reactions on micelle, and also for long-range interactions.

Acknowledgment. The authors would like to thank the National Science Foundation for support of this work via Grant No. CHE 82-01226. Our thanks are also due to Mr. James Wheeler for writing the computer programs used to fit the experimental data. We are grateful to the reviewers for valuable comments.

Registry No. NaLS, 151-21-3; $Ru(bpy)_3^{2+}$, 74391-32-5; Cu^{2+} , 15158-11-9; Cr^{3+} , 16065-83-1; Fe^{3+} , 20074-52-6; $C_{16}C_2V^{2+}$, 78769-77-4; ethylene glycol, 107-21-1; pyrene, 129-00-0.

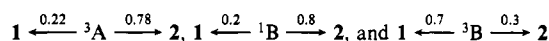
(28) The reaction of singlet pyrene with Ag^+ or Tl^+ is known to result in the intersystem crossing of pyrene. See, for example: Geacintov, N. E.; Prusik, T.; Khosrofi, M. *J. Am. Chem. Soc.* **1976**, *98*, 6444. Nosaka, Y.; Kira, A.; Imamura, M. *J. Phys. Chem.* **1981**, *85*, 1353.

Spin Inversion in the 1,4-Diradical Derived from 2,4,6-Triisopropylbenzophenone: Importance of Lone-Pair Orbital Rotation

Yoshikatsu Ito* and Teruo Matsuura

Contribution from the Department of Synthetic Chemistry, Faculty of Engineering, Kyoto University, Kyoto 606, Japan. Received June 28, 1982

Abstract: 4,6-Diisopropyl-2,2-dimethyl-1-phenyl-1,2-dihydrobenzocyclobuten-1-ol (**2**) was submitted to direct (254 nm) and sensitized photolysis and thermolysis in the absence or presence of oxygen. Direct photolysis (313 nm) of 2,4,6-triisopropylbenzophenone (**1**) was also performed in the absence or presence of oxygen. Interconversion between **1** and **2** and production of 1,3-diisopropyl-10,10-dimethylanthrone (**3**) and 1,4-dihydro-1-hydroxy-6,8-diisopropyl-4,4-dimethyl-1-phenyl-2,3-benzodioxin (**4**) happened in various quantum yields depending upon the reaction conditions. For example, the quantum yield of the transformation **2** → **1** was greatly different between direct ($\Phi = 0.2$) and triplet-sensitized ($\Phi = 0.7$, a limiting value) photolysis of **2**. It is deduced from analysis of measured product distributions ($\Phi(1)$ vs. $\Phi(2)$) that quantum efficiencies for partitioning of a diradical intermediate DR are



where A (two face-to-edge odd orbitals) and B (two face-to-face odd orbitals) are different conformations of the same diradical species DR. This result led us to conclude that rotation of the lone-pair orbital in the diradical DR may create an effective vibrational overlap (Franck-Condon factor), leading to an efficient intersystem crossing of the diradical. It is also concluded that DR, which is generated from the direct photolysis of **1**, is spin protected and its lifetime is determined by the rate of intersystem crossing. The oxygen-trapping experiment indicated an unusually slow rate constant for reaction between DR and oxygen ($k_0' = 3.0 \times 10^7 \text{ M}^{-1} \text{ s}^{-1}$).

Diradical chemistry is an active area of research both theoretically and experimentally. The most well-studied diradical

species that are frequently encountered in organic reactions as unstable intermediates include type II diradicals,² Paterno-Büchi

Table I. Quantum Yields for Direct Photolyses of 2 and 1

expt	reactant (M)	solvent	irrad wave-length, nm	quantum yields ^a		
				$\Phi(1)$	$\Phi(3)^b$	$\Phi(4)$
1	2 (0.05)	hexane	254	0.19	~0.01	0
2	2 (0.10)	hexane	254	0.22	~0.01	0
3	2 (0.20)	hexane	254	0.23	~0.01	0
4	2 (0.05)	methanol	254	0.17	~0.01	0
5	2 (0.05)	acetonitrile	254	0.21	~0.01	0
6	2 (0.05)	hexane ^c	254	0.20	~0.01	0.031
7	1 (0.05)	benzene	313	0.60 ^{d,e}	~0.0001 ^f	0
8	1 (0.05)	benzene ^g	313	0.45 ^d	nd ^h	0.022

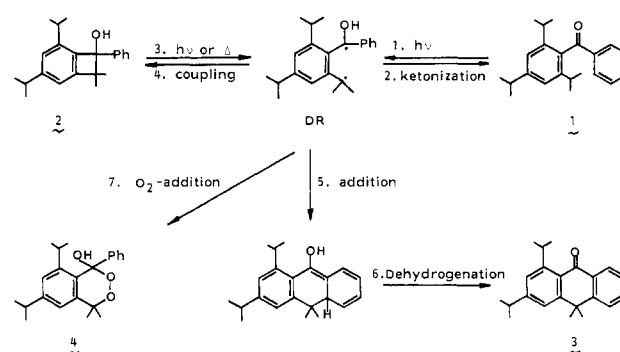
^a Maximum experimental error, $\pm 10\%$. ^b Variable ($\pm 50\%$) for different runs. ^c O₂ saturated. ^d $\Phi(2)$. ^e The data in ref 15. ^f Almost invariant with the extent of conversion of 1 (5–100%). ^g Air saturated. ^h Not determined.

diradicals,³ type I diradicals,⁴ trimethylenemethane diradicals,⁵ *o*-xylenes (a typical diradicaloid hydrocarbon),⁶ and so forth.⁷ In particular various methods and compounds are available for generating the *o*-xylenes, which are very useful for both synthetic⁸ and mechanistic study⁹ applications. For example, loss of CO, N₂, or SO₂ from suitable cyclic compounds, photochemical internal hydrogen abstraction of *o*-alkyl aromatic ketones (photoenolization), and thermolysis or photolysis of benzocyclobutenes are among them.⁶

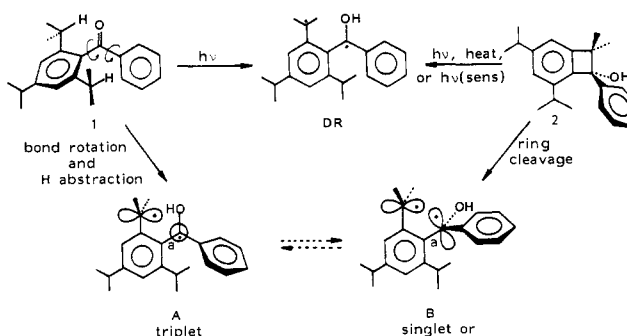
By nature the fundamental properties of diradicals such as the lifetime, reactivity, intersystem crossing rate, singlet–triplet energy separation, and electronic (diradical or ionic) character should be very sensitive to the diradical geometries, since the Coulomb and exchange integrals between two odd electrons vary rapidly with change in the orbital conformation.¹⁰ In 1972 Salem reported useful theory which provides several geometric factors required for an efficient diradical intersystem crossing to occur.^{10a} Since then several experimental and theoretical verifications for this theory have been presented mainly by Turro and Epiotis.¹¹ It is evident, however, that the main difficulty in these problems resides in finding an appropriate diradical system whose geometrical changes during the lifetime can be traced by some means (chemical trapping, laser spectroscopy, CIDNP, ESR, etc.).

Berson et al. failed to capture separately the planar and bisected trimethylenemethane diradicals even by use of the most reactive trapping reagents.¹² Very recently Scaiano has implicated a decisive role of triplet diradical conformations in determining the product distributions of Norrish type II reactions.¹³ Kaptein and

Scheme I



Scheme II



- (1) Photoinduced Reactions. 143.
- (2) Scaiano, J. C.; Lissi, E. A.; Encinas, M. V. *Rev. Chem. Intermed.* **1978**, *2*, 139.
- (3) (a) Freilich, S. C.; Peters, K. S. *J. Am. Chem. Soc.* **1981**, *103*, 6255. (b) Caldwell, R. A.; Majima, T.; Pac, C. *Ibid.* **1982**, *104*, 629.
- (4) (a) Closs, G. L.; Miller, R. J. *J. Am. Chem. Soc.* **1981**, *103*, 3586. (b) Baulch, D. L.; Colburn, A.; Lenney, P. W.; Montague, D. C. *J. Chem. Soc., Faraday Trans. 1* **1981**, *77*, 1803.
- (5) (a) Berson, J. A. *Acc. Chem. Res.* **1978**, *11*, 446. (b) Feller, D.; Davidson, E. R.; Borden, W. T. *J. Am. Chem. Soc.* **1982**, *104*, 1216.
- (6) (a) McCullough, J. J. *Acc. Chem. Res.* **1980**, *13*, 270. (b) Oppolzer, W. *Synthesis* **1978**, 793.
- (7) Berson, J. A. "Rearrangements in Ground and Excited States"; de Mayo, P., Ed.; Academic Press: New York, 1980; Vol. 1, p 311.
- (8) (a) Funk, R. L.; Vollhardt, K. P. C. *Chem. Soc. Rev.* **1980**, *9*, 41. (b) Kametani, T.; Suzuki, K.; Nemoto, H. *J. Am. Chem. Soc.* **1981**, *103*, 2890. (c) Ito, Y.; Nakatsuka, M.; Saegusa, T. *Ibid.* **1981**, *103*, 476.
- (9) (a) Dolbier, W. R., Jr.; Matsue, K.; Dewey, H. J.; Horak, D. V.; Michl, J. *J. Am. Chem. Soc.* **1979**, *101*, 2136. (b) Tseng, K. L.; Michl, J. *Ibid.* **1977**, *99*, 4840.
- (10) (a) Salem, L.; Rowland, C. *Angew. Chem., Int. Ed. Engl.* **1972**, *11*, 92. (b) Borden, W. T.; Davidson, E. R. *Annu. Rev. Phys. Chem.* **1978**, *30*, 125.
- (11) (a) Turro, N. J.; Devaquet, A. *J. Am. Chem. Soc.* **1975**, *97*, 3859. (b) Turro, N. J.; Ramamurthy, V.; Liu, K. C.; Krebs, A.; Kemper, R. *Ibid.* **1976**, *98*, 6758. (c) Turro, N. J.; Chow, M.; Ito, Y. *Ibid.* **1978**, *100*, 5580. (d) Turro, N. J.; Cherry, W. R.; Mirbach, M. F.; Mirbach, M. J. *Ibid.* **1977**, *99*, 7388. (e) Shaik, S. S.; Epiotis, N. D. *Ibid.* **1980**, *102*, 122 and references cited therein. (f) Larson, J. R.; Epiotis, N. D.; McMurchie, L. E. *J. Org. Chem.* **1980**, *45*, 1388.
- (12) Cichra, D. A.; Duncan, C. D.; Berson, J. A. *J. Am. Chem. Soc.* **1980**, *102*, 6527.
- (13) Scaiano, J. C. *Tetrahedron* **1982**, *38*, 819.

Kaptein have shown from an analysis of magnetic-field-dependent CIDNP effects that cyclization of the cyclohexanone type I diradical into the parent cyclohexanone molecule takes place directly from the triplet diradical state via *p*-orbital rotation,¹⁴ although it remains possible that the CIDNP effects arose from very small fractions of the total reaction.

In the previous paper¹⁵ we have reported a quantitative photochemical transformation of 2,4,6-triisopropylbenzophenone (1) to the corresponding benzocyclobutenol 2 via a diradical intermediate DR (path 1 → 4 in Scheme I). This reaction has an advantage in the study of diradical chemistry, because DR may also be produced by photolysis or thermolysis of 2 (reaction 3 in Scheme I).^{6b,18f} As illustrated in Scheme II, the ketone 1¹⁵ and the cyclobutenol 2 are expected to generate the same diradical (DR) with different conformations (A and B, respectively) and with defined spin multiplicities (singlet or triplet), thus allowing the study of spin-state and geometry effects upon reactions associated with the photoenol-type diradicals.

We will now show evidence (1) that the triplet diradical ³DR, which is generated by photolysis of 1, is really spin protected and its lifetime is controlled by the T–S intersystem crossing and (2) that rotation of a lone-pair orbital in DR induces a favorable

(14) de Kanter, F. J. J.; Kaptein, R. *J. Am. Chem. Soc.* **1982**, *104*, 4759.

(15) Ito, Y.; Nishimura, H.; Umehara, Y.; Yamada, Y.; Tone, M.; Matsuura, T. *J. Am. Chem. Soc.* **1983**, *105*, 1590.

Table II. Quantum Yields for Sensitized Photolyses of the Cyclobutenol **2** and Valerophenone

expt	reactant (M)	solvent	sensitizer	E_T^a kcal/mol	irrad wave- length, nm	$\Phi(1)^b$
1	2 (0.10)	benzene	benzene	84.3	254	0.37
2	2 (0.0011)	hexane	benzene (0.11 M)	84.3	254	0.11
3	2 (0.10)	anisole	anisole	80.8	254	0.11
4	2 (0.10)	acetone	acetone	79–82	313	0.48
5	2 (0.083)	benzene	acetophenone (0.079 M)	74.1	313	0.009 ^c
6	valerophenone (0.0021)	hexane	benzene (0.11 M)	84.3	254	0.15 ^d

^a Murov, S. L. "Handbook of Photochemistry"; Marcel Dekker: New York, 1975. ^b Maximum experimental error, $\pm 10\%$. ^c Reference 20d. ^d Φ (acetophenone).

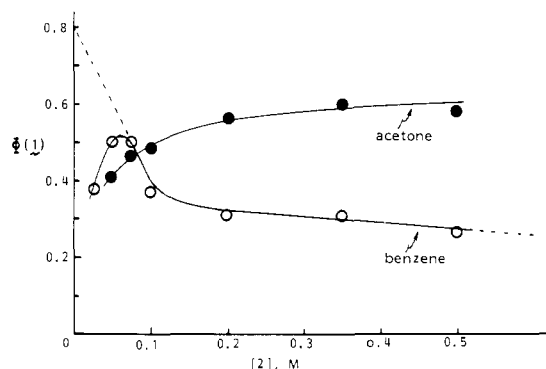


Figure 1. Quantum yields for 2,4,6-triisopropylbenzophenone (**1**) formation from benzene (solvents)- or acetone (solvent)-sensitized photolyses, plotted as a function of concentration of the cyclobutenol **2**. Irradiations were carried out at 254 nm (for benzene sensitization) or at 313 nm (for acetone sensitization).

Franck-Condon overlap, leading to an efficient mixing of the singlet and triplet diradical states.

Results and Discussion

Direct Photolyses. Direct photolysis (254 nm) of a degassed solution of the benzocyclobutenol **2** resulted in moderately efficient formation ($\Phi = 0.17$ – 0.23) of 2,4,6-triisopropylbenzophenone (**1**). In addition 1,3-diisopropyl-10,10-dimethylantrone (**3**) was inefficiently formed ($\Phi \sim 0.01$). The product quantum yields are summarized in Table I (experiments 1–5). It can readily be seen from the table that the quantum yield of **1** is nearly independent of both the concentration of **2** (0.05–0.20 M) and the solvent employed (hexane, methanol, and acetonitrile). The Φ values for formation of **3** were rather erratic, indicating a complex mechanism for dehydrogenation.¹⁶ In each case the reaction was stopped at a very low conversion ($< 0.1\%$).¹⁷ In a separate experiment the product balance was found to be excellent ($> 90\%$) even after prolonged irradiation.

As shown in the preceding paper,¹⁵ the photocyclization of **1** to the cyclobutenol **2** proceeded quantitatively with high efficiency. However, closer examination of a photolysate revealed that the anthrone **3** was also formed in a minimal yield ($\Phi \sim 0.0001$, experiment 7).

Irradiation (254 nm) of **2** in hexane saturated with O_2 gave an oxygen cycloadduct **4** along with **1** and **3** (experiment 6). Similarly, photolysis (313 nm) of **1** in air-saturated benzene produced the adduct **4** along with the cyclobutenol **2** (experiment 8). This reaction was already reported.^{20e} It is known that O_2 is the best chemical trap for triplet *o*-xylene.¹⁸

(16) The transformation of **2** into **3** involves a dehydrogenation step (reaction 6 in Scheme I). The exact mechanism for the dehydrogenation is uncertain, but it was confirmed that $\Phi(3)$ was not affected by the presence or absence of oxygen during the photolysis; compare experiments 1 and 6 in Table I, for example. It was also confirmed that the product composition of the photolysate was unchanged in the dark for several days, even if it was exposed to air.

(17) In the photolyses of **2** throughout this paper, the reactions were stopped at a very low conversion in order to suppress the effect of the back photoreaction from **1** to **2**.¹⁵

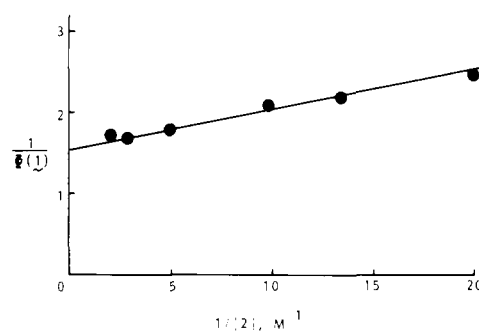


Figure 2. Double reciprocal plot of the acetone-sensitization data in Figure 1.

Table III. Chemical Yields for Thermolysis of **2** (0.021 M) in *tert*-Butylbenzene

expt	conds for thermolysis	chemical yields, %			conv of 2 , %
		1	3	4	
1	135 °C, 4 h ^a	99	0.08	0	49
2	134 °C, 4 h ^b	89	0.02	0.1	40

^a Under N_2 bubbling. ^b Under O_2 bubbling.

Sensitized Photolyses of **2.** The transformation of **2** into **1** could also be effected by means of several triplet sensitizers. Quantum yields $\Phi(1)$ obtained from sensitized photolysis of a degassed solution under various conditions are summarized in Table II (experiments 1–5) and Figure 1.¹⁷ As in the direct photolysis of **2** (Table I), the anthrone **3** was always formed as a byproduct with a very low efficiency ($\Phi(3) \sim 0.005$).

Table II demonstrates that triplet sensitizers with energies $E_T > 79$ kcal/mol (benzene, anisole, acetone) have sufficient excitation energy to sensitize the reaction $2 \rightarrow 1$. Since, as will be shown later,^{23,25} the rate for triplet-triplet energy transfer from

(18) (a) Haag, R.; Wirz, J.; Wagner, P. J. *Helv. Chim. Acta* **1977**, *60*, 2595. (b) Small, R. D., Jr.; Scaiano, J. C. *J. Am. Chem. Soc.* **1977**, *99*, 7713. (c) Findlay, D. M.; Tchir, M. F. *J. Chem. Soc., Faraday Trans. 1* **1976**, *72*, 1096. (d) Lutz, H.; Breheret, E.; Lindqvist, L. *Ibid.* **1973**, *69*, 2096. (e) Carre, M.; Viriot-Villaume, M.; Caubere, P. *J. Chem. Soc., Perkin Trans. 1* **1979**, 2542. (f) Viriot-Villaume, M.; Carre, M.; Caubere, P. *Ibid.* **1979**, 1395.

(19) Thermolysis of **2** in toluene at 160 °C under a high pressure of oxygen (30 atm) increased the yield of **4** to 9% (Ito, Y.; Nishimura, H.; Matsuura, T., unpublished result.)

(20) (a) Ito, Y.; Umehara, Y.; Hijiya, T.; Yamada, Y.; Matsuura, T. *J. Am. Chem. Soc.* **1980**, *102*, 5917. (b) Ito, Y.; Nishimura, H.; Matsuura, T.; Hayashi, H. *J. Chem. Soc., Chem. Commun.* **1981**, 1187. (c) Hayashi, H.; Nagakura, S.; Ito, Y.; Matsuura, T. *Chem. Lett.* **1980**, 939. (d) Ito, Y.; Giri, B. P.; Nakasuiji, M.; Hagiwara, T.; Matsuura, T. *J. Am. Chem. Soc.* **1983**, *105*, 1117. (e) Kitaura, Y.; Matsuura, T. *Tetrahedron* **1971**, *27*, 1597.

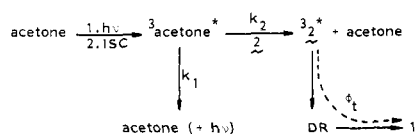
(21) (a) Barltrop, J. A.; Coyle, J. D. *Tetrahedron Lett.* **1968**, 3235. (b) Wagner, P. J. *Ibid.* **1968**, 5385.

(22) (a) Wagner, P. J.; Kelso, P. A.; Kemppainen, A. E.; McGrath, J. M.; Schott, H. N.; Zepp, R. G. *J. Am. Chem. Soc.* **1972**, *94*, 7506. (b) Wagner, P. J.; Kochevar, I. E.; Kemppainen, A. E. *Ibid.* **1972**, *94*, 7489. (c) Wagner, P. J.; Kochevar, I. E. *Ibid.* **1968**, *90*, 2232.

(23) One calculates $k_q = 2.8 \times 10^7 \text{ M}^{-1} \text{ s}^{-1}$, assuming that the decay rate of triplet acetone (τ^{-1}) in acetonitrile is $1.7 \times 10^4 \text{ s}^{-1}$.²⁴

(24) Wilson, T.; Halpern, A. M. *J. Am. Chem. Soc.* **1980**, *102*, 7279.

Scheme III



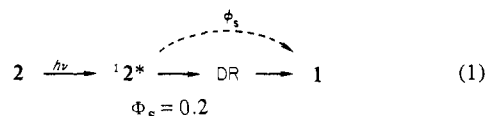
acetone to **2** is two to three orders of magnitude slower than the diffusion rate, the triplet energy of the cyclobutenol **2** appears to be 82–84 kcal/mol.

It was found by varying the concentration of **2** (0.025–0.5 M, Figure 1) that $\Phi(1)$ obtained from sensitization with the solvent acetone increased with the increase in **[2]**, while $\Phi(1)$ obtained from sensitization with the solvent benzene gradually decreased at higher **[2]** and had a maximum at around 0.07 M of **2**. It is noticeable that the highest $\Phi(1)$ value thus obtained from sensitization with either benzene ($\Phi(1) = 0.50$) or acetone ($\Phi(1) = 0.60$) far exceeded the values from direct photolysis (Table I, $\Phi(1) = 0.17$ – 0.23). The data for acetone sensitization gave a good linear plot of $\Phi(1)^{-1}$ vs. reciprocal concentration of **2** (Figure 2).

Thermolyses of 2. The ring opening of **2** into **1** was also achieved thermally in *tert*-butylbenzene in the absence or presence of oxygen (Table III). Despite a very low yield **3** (and **4**)¹⁹ was (were) also formed.

Reaction Pathways. Scheme I shows the most economical reaction sequence capable to accommodate all the materials **1**–**4** described above. The diradical DR is a key intermediate in this scheme.

Product Distribution from 2 of Different Multiplicities. Lack of solvent dependence in $\Phi(1)$ upon direct photolysis of **2** (experiments 1, 4, and 5 in Table I) is reminiscent of the Norrish type II reaction from the singlet states of acyclic alkyl ketones, where the quantum yields for reaction from S_1 do not depend on solvent polarity.²¹ Lack of concentration dependence in $\Phi(1)$ (experiments 1–3 in Table I) also suggests²² that the direct photolysis occurs from the singlet state of **2**. In fact, the production of both **1** and **3** from the cyclobutenol **2** in hexane was never quenched by addition of piperylene up to 0.1 M concentration. Hence we concluded from the measured $\Phi(1)$ values (Table I, experiments 1–5) that the quantum efficiency for the formation of **1** from the singlet state of **2** (Φ_s) was 0.2 ± 0.03 (eq 1).

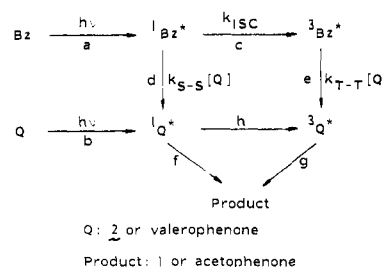


Evidently the triplet state of acetone is involved in the acetone-photosensitized process of **2**, since the acetone phosphorescence at room temperature (0.036 M acetone in degassed acetonitrile) was quenched by **2** with high efficiency ($k_q\tau = 1660 \pm 30 \text{ M}^{-1}$),²³ while the acetone fluorescence was totally unaffected by additions of **2** up to 0.1 M. Thus, on the basis of the usual triplet-triplet energy transfer mechanism (Scheme III) and the kinetic expression derived from this scheme (eq 2), the observed linear plot of Figure 2 (intercept = 1.5, intercept/slope = 32 M^{-1}) was interpreted.²⁵ It was estimated from the intercept ($=\Phi_t^{-1}$) that the quantum efficiency for the formation of **1** from the triplet state of **2** (Φ_t) was 0.67.

$$\Phi(1)^{-1} = \Phi_t^{-1} \left(1 + \frac{k_1}{k_2[2]} \right) \quad (2)$$

The gradual decrease in $\Phi(1)$ at higher cyclobutenol concentrations in the benzene-sensitized photolyses of **2** (Figure 1) can be ascribed to two factors. First, both the S_1 and T_1 energy levels of benzene will be high enough to transfer its electronic energy

Scheme IV



to **2**. Therefore the interception by **2** of S_1 benzene prior to its intersystem crossing to the T_1 state is expected to occur at higher **[2]**. Second, the competitive absorption of incident light (254 nm wavelength) by **2** and benzene ($\epsilon_2 = 988 \text{ M}^{-1} \text{ cm}^{-1}$ and $\epsilon_{\text{benzene}} = 179 \text{ M}^{-1} \text{ cm}^{-1}$ at 254 nm) becomes important at higher **[2]**.²⁷ As a result of these two effects, the singlet reaction will become predominant over the triplet reaction as **[2]** increases. In fact, it can be seen from Figure 1 that the $\Phi(1)$ value tends to approach to that of the direct photolysis ($\Phi(1) \sim 0.2$, Table I) as **[2]** increases. The abrupt change in $\Phi(1)$ at lower concentrations of **2** (0.025–0.05 M, Figure 1) suggests that the triplet-triplet energy transfer from benzene to **2** is nearly diffusion controlled, since the triplet lifetime of pure liquid benzene is very short (a few nanoseconds).^{28b}

Since the photophysics of benzene in the solution phase is more precisely understood in a dilute solution than in neat benzene,²⁸ the use of low concentration benzene as a photosensitizer is more suitable for a detailed kinetic analysis (experiment 2 in Table II). In this experiment 0.11 M benzene in hexane was used. Scheme IV shows the most probable reaction mechanism. Most of the incident light (95%)²⁹ was absorbed by benzene (Bz) under the reaction conditions with some competitive absorption (5%) by **2** ($=Q$). The excited singlet benzene ($^1\text{Bz}^*$) causes the product (**1**) formation either through singlet-singlet energy transfer to **2** (path d \rightarrow f) or through intersystem crossing followed by triplet-triplet energy transfer to **2** (path c \rightarrow e \rightarrow g). The singlet to triplet intersystem crossing of **2** (step h) can be neglected (refer to the first paragraph of this section). Thus the quantum yield for **1** can be expressed by eq 3, where the symbol Φ with the subscripts c–g denote the quantum efficiency of each step in Scheme IV.

$$\Phi(1) = 0.95(\Phi_d\Phi_f + \Phi_c\Phi_e\Phi_g) + 0.05\Phi_f \quad (3)$$

It can readily be derived from the usual steady-state treatment that

$$\begin{aligned} \Phi_c &= \Phi_T / (1 + k_{S-S}\tau_S[Q]) \\ \Phi_d &= k_{S-S}\tau_S[Q] / (1 + k_{S-S}\tau_S[Q]) \\ \Phi_e &= k_{T-T}[Q] / (\tau_T^{-1} + k_{T-T}[Q]) \end{aligned} \quad (4)$$

where τ_S , τ_T , and $\Phi_T (=k_{ISC}\tau_S)$ denote the singlet lifetime, the triplet lifetime, and the intersystem crossing yield for benzene in the absence of **2**, respectively. The fluorescence of benzene (0.11 M) in hexane was found to be quenched by **2** with $k_{S-S}\tau_S = 200 \text{ M}^{-1}$ (Figure 3); $\Phi_f (= \Phi_s)$ is already known (eq 1). Thus if we know the values of τ_T , Φ_T , and k_{T-T} , the value of $\Phi_g (= \Phi_t)$ can be calculated from eq 3 and 4, since $\Phi(1) = 0.11$ and $[Q] = 0.0011 \text{ M}$ (experiment 2 in Table II).

The photophysics of benzene is well studied²⁸ and it is established that $\Phi_T \sim 0.24$ at low concentrations ($\sim 0.1 \text{ M}$) in hydrocarbon solvents.³⁰ However, the triplet lifetime τ_T (21 ns),

(26) Borkman, R. F.; Kearns, D. R. *J. Am. Chem. Soc.* **1966**, *88*, 3467.

(27) In the case of the acetone sensitization experiments (Figure 1) the incident light (313 nm) was exclusively absorbed by the sensitizer ($\epsilon_{\text{acetone}} = 3 \text{ M}^{-1} \text{ cm}^{-1}$ and $\epsilon_2 = 0.05 \text{ M}^{-1} \text{ cm}^{-1}$ at 313 nm).

(28) (a) Cundall, R. B.; Robinson, D. A.; Pereina, L. C. *Adv. Photochem.* **1977**, *10*, 147. (b) Cundall, R. B.; Ogilvie, S. M. "Organic Molecular Photochemistry"; Birks, J. B.; Ed.; Wiley: New York, 1975; Vol. 2, p 33.

(29) From $\epsilon_{\text{Bz}}[\text{Bz}] / (\epsilon_{\text{Bz}}[\text{Bz}] + \epsilon_2[\text{2}])$ at 254 nm.

(25) From the value of intercept/slope ($=k_2/k_1$) and the reported value for k_1 ($2 \times 10^6 \text{ s}^{-1}$),²⁶ one calculates $k_2 = 6 \times 10^7 \text{ M}^{-1} \text{ s}^{-1}$. The observation that k_2 is fairly close to k_q determined from phosphorescence quenching²³ substantiates the mechanism described in Scheme III.

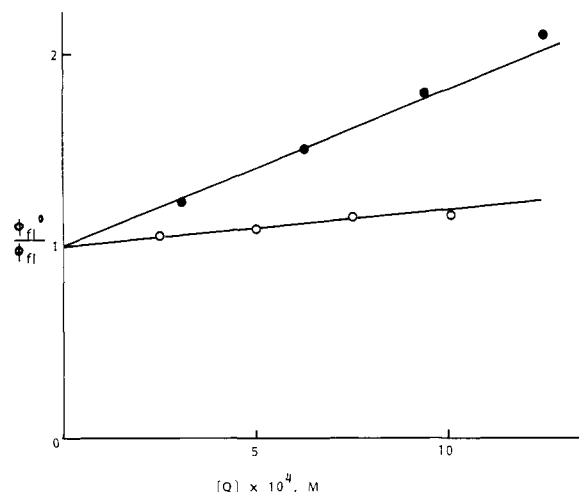
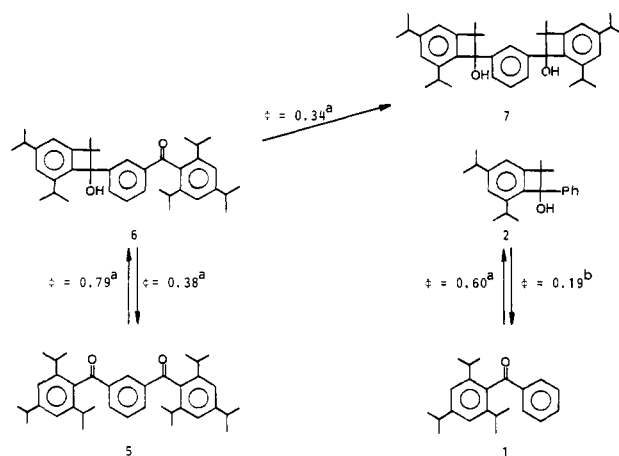


Figure 3. Fluorescence quenching of benzene (0.11 M) by the benzocyclobutenol **2** (O) or valerophenone (●) in hexane ($\lambda_{exc} = 255 \pm 5$ nm). The data were corrected for competitive absorption of light with use of the following average extinction coefficients in the region 255 ± 5 nm: $\epsilon_{Bz} = 97 \text{ M}^{-1} \text{ cm}^{-1}$, $\epsilon_2 = 935 \text{ M}^{-1} \text{ cm}^{-1}$, $\epsilon_{PhCOBu} = 765 \text{ M}^{-1} \text{ cm}^{-1}$.

Scheme V



^a Irradiated at 313 nm in benzene (0.05 M).^{20d}

^b Irradiated at 254 nm in hexane (0.05 M) (Table I, experiment 1).

which was determined by the benzene (0.112 M)-sensitized *cis*,*trans* isomerization of *cis*-2-butene in cyclohexane,³¹ seems to require re-estimation for our purpose. Thus benzene (0.11 M in hexane)-sensitized photolysis of valerophenone was performed and the quantum yield of acetophenone formation was determined (experiment 6 in Table II). Since the Norrish type II reaction of valerophenone is well studied,²² the triplet lifetime of benzene can be readily evaluated from the $\Phi(\text{acetophenone})$ value on the basis of the mechanism described in Scheme IV and hence eq 5.³²

$$\Phi(\text{acetophenone}) = 0.95(\Phi_d\Phi_h + \Phi_c\Phi_e)\Phi_g + 0.05\Phi_h\Phi_g \quad (5)$$

The singlet reaction (reaction f) does not occur in this case.²² The fluorescence of benzene (0.11 M) in hexane was quenched by valerophenone with $k_{S-S\tau_S} = 800 \text{ M}^{-1}$ (Figure 3). The quantum yield of acetophenone formation from direct photolysis (254 nm)

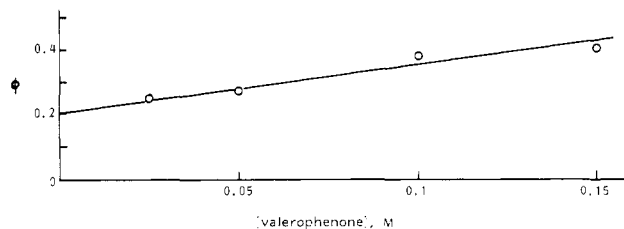
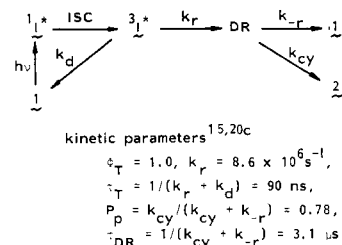


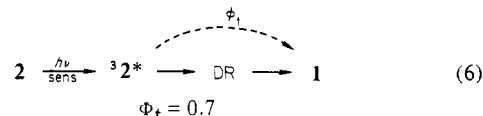
Figure 4. Quantum yield of acetophenone formation from valerophenone as a function of valerophenone concentration in hexane, irradiated at 254 nm.

Scheme VI



of valerophenone (0.0021 M) in hexane was estimated to be 0.21 by extrapolation of the values at higher concentrations (Figure 4).³³ Using these prerequisite data and assuming that the rate of the triplet energy transfer from benzene to valerophenone is diffusion controlled ($k_{T-T} = 1.1 \times 10^{10} \text{ M}^{-1} \text{ s}^{-1}$ in hexane^{22c}), we estimated the triplet lifetime of benzene (τ_T) as 69 ns in a dilute hexane solution (0.11 M) at 25 °C.

On the basis of the above photokinetic data associated with benzene, i.e., $\Phi_T = 0.24$ and $\tau_T = 69 \text{ ns}$, and on the assumption that the rate constant for triplet-triplet energy transfer (k_{T-T}) from benzene triplet to **2** is diffusion controlled ($1.1 \times 10^{10} \text{ M}^{-1} \text{ s}^{-1}$ in hexane^{22c}), $\Phi_g (= \Phi_i)$ was estimated from eq 3 and 4 as 0.77. The value estimated from the acetone sensitization experiments (Figure 2) was 0.67. Hence we concluded that the Φ_i value is 0.7 ± 0.1 (eq 6). It should be noted that the quantum efficiency for the



ring opening $2 \rightarrow 1$ is much higher from the triplet manifold (0.7, eq 6) than from the singlet manifold (0.2, eq 1).

Further confirmation of this remarkable multiplicity effect on the reaction $2 \rightarrow 1$ comes from the result of the recently published^{20d} photointerconversion of meta benzoyl-substituted homologues, $5 \rightleftharpoons 6$ (Scheme V). It is clear from Scheme V that **5** undergoes photocyclization to **6** with good efficiency ($\Phi = 0.79$), slightly superior to that for the reaction $1 \rightarrow 2$ ($\Phi = 0.60$), while the quantum yield for the back photoreaction $6 \rightarrow 5$ ($\Phi = 0.38$) is twice that of $2 \rightarrow 1$ ($\Phi = 0.19$). Furthermore, if we correct for the energy loss of the excited molecule **6** by another photochemical route $6 \rightarrow 7$ ($\Phi = 0.34$), the quantum yield of $6 \rightarrow 5$ is at least 0.58 (from $0.38/(1.0 - 0.34) = 0.58$), resulting in three times that of $2 \rightarrow 1$. This big difference in the quantum yield, $\Phi(6 \rightarrow 5) \gg \Phi(2 \rightarrow 1)$, is probably attributed to the multiplicity difference of the responsible excited states, since it is established that the reaction $6 \rightarrow 5$ is from the triplet state^{20d} and the reaction $2 \rightarrow 1$ is from the singlet state (vide supra).

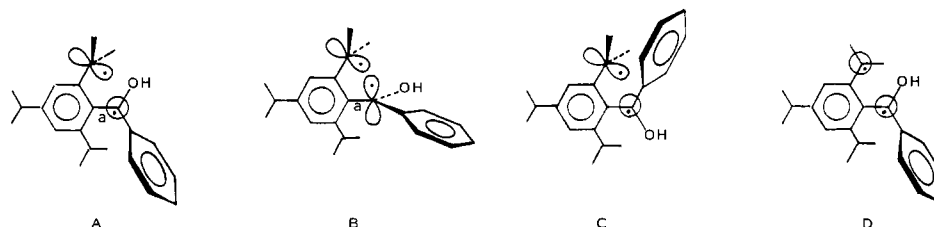
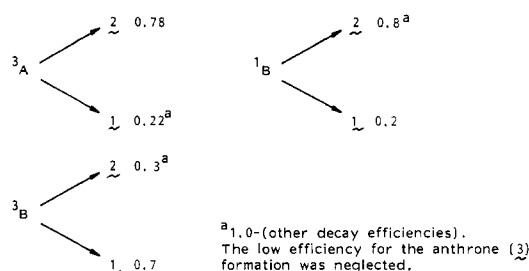
Product Distribution from DR of Different Multiplicities and Conformations. Figure 5 (A–D) illustrates four idealized conformations of the diradical intermediate DR.³⁴ In conformations

(30) The Φ_T value for benzene is known to be concentration dependent, e.g., ~ 0.6 for neat benzene.²⁸

(31) Cundall, R. B.; Robinson, D. A. *J. Chem. Soc., Faraday Trans. 2* **1972**, 68, 1145.

(32) Based on $\epsilon_{Bz}[Bz]/(\epsilon_{Bz}[Bz] + \epsilon_{valerophenone}[valerophenone])$, 95% of incident light (254 nm) was absorbed by benzene ($\epsilon_{Bz} = 179 \text{ M}^{-1} \text{ cm}^{-1}$ and $\epsilon_{valerophenone} = 500 \text{ M}^{-1} \text{ cm}^{-1}$ at 254 nm). The quantum efficiencies Φ_c , Φ_d , and Φ_g can be represented by eq 4, where Q is valerophenone. Φ_h is equal to 1.²² It was found that $\Phi(\text{acetophenone}) = 0.15$ (experiment 6 in Table II) and $\Phi_g = 0.21$ (Figure 4).

(33) A similar concentration dependence was observed when irradiated at 313 nm in benzene.^{22b}

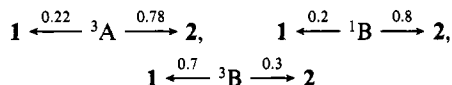
**Figure 5.** Four idealized conformations of the diradical DR.**Scheme VII**

A and C the two odd orbitals are directed at right angles to each other, whereas in B they are coplanar and in D they are parallel. The molecules 1 and 2 are expected to be potential precursors to the structures A and B, respectively (Scheme II). As will be shown later, the interconversion of A and B by rotation around bond a is crucial for understanding the behavior of DR.

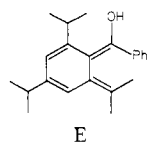
The anthrone 3 may be assumed to be formed via the conformation C. However, since 3 is merely a minor product as described above, we will not discuss its formation mechanism in detail. It is unlikely that the highly crowded diradical DR will take the conformation D, since it has a strong steric repulsion due to the bulky ortho substituents.

In the previous paper¹⁵ we have shown that the diradical DR at the moment of generation from the direct photolysis of the ketone 1 is in its triplet state and has a conformation near A (³A), leading to formation of the cyclobutenol 2 with high efficiency, i.e., $P_p = k_{cy}/(k_{cy} + k_r) = 0.78$ (Scheme VI). This and the data described in eq 1 and 6 eventually led us to know the probabilities for formation of the final products 1 and 2 from either ³A, ¹B, or ³B as summarized in Scheme VII, where the generation of B from 2 is assumed to occur with unit quantum efficiency from both the direct and sensitized excitation of 2.³⁵

Intersystem Crossing (ISC) in the Diradical DR. The triplet diradical conformer ³A and ³B must flip spin into the singlet state before collapse to the molecular products 1 and 2. The data in Scheme VII

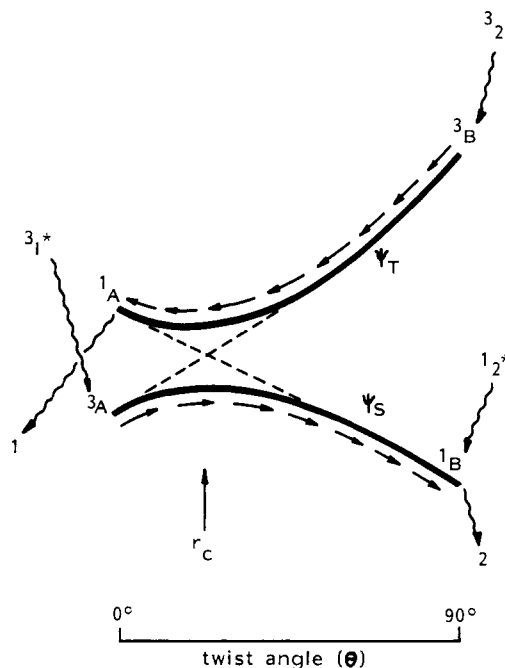


(34) In this paper we do not differentiate the diradical DR (planar or twisted, singlet or triplet) from the enol-type structure E (planar or twisted, singlet or triplet), since it is known that *o*-xylenes are typical diradicaloid hydrocarbons.⁶ Therefore, the structures A–D may be represented as the



corresponding enols of the same geometry and spin state. We consider that E species described previously as dienols (or enols) which were detected by laser spectroscopy or trapped by dienophiles upon photolyses of several *o*-alkyl phenyl ketones^{18,37} probably best correspond to the planar conformer D. Likewise, species described previously as diradicals (or triplet enols)^{18,37} probably refer to the twisted conformers A and C.

(35) Professor P. J. Wagner, however, points out that this assumption as well as the uncertain contribution of enol (or D³⁴) formation to quantum efficiencies clouds the following conclusion somewhat.

**Figure 6.** A hypothetical energy surface of the lowest triplet (Ψ_T) and the lowest singlet (Ψ_S) states of the diradical DR. The geometry of DR is varied from A ($\theta = 0^\circ$) to B ($\theta = 90^\circ$) by the rotation around bond a (see Figure 5).

led us to conclude (1) that there is no conformational equilibrium between ³A and ³B during the lifetime of DR, since they gave different product distributions,³⁶ (2) that the ISC occurring concomitantly with the conformational change (p-orbital rotation), i.e., ³A → ¹B, is efficient, since a similar product distribution was obtained from either ³A or ¹B, and (3) that the ISC without a simultaneous p-orbital rotation, i.e., ³B → ¹B, is inefficient, since the product distributions from ³B and ¹B were completely different from each other.³⁸

These three conclusions are readily rationalized by an avoidance of the zero-order surface crossing of the singlet and triplet diradical states (solid line in Figure 6). In this figure a hypothetical energy surface connecting the two conformations A and B of DR is illustrated. It is assumed from consideration of the magnitude of an overlap integral between the two lone-pair orbitals in the conformation A or B that ³A is lower in energy than ¹A (a small overlap case), while ³B is higher than ¹B (a large overlap case).^{10a} A similar energy diagram was presented for the photoenolization of *o*-methylacetophenone^{18a} and a model system.⁴⁰ Thus the main

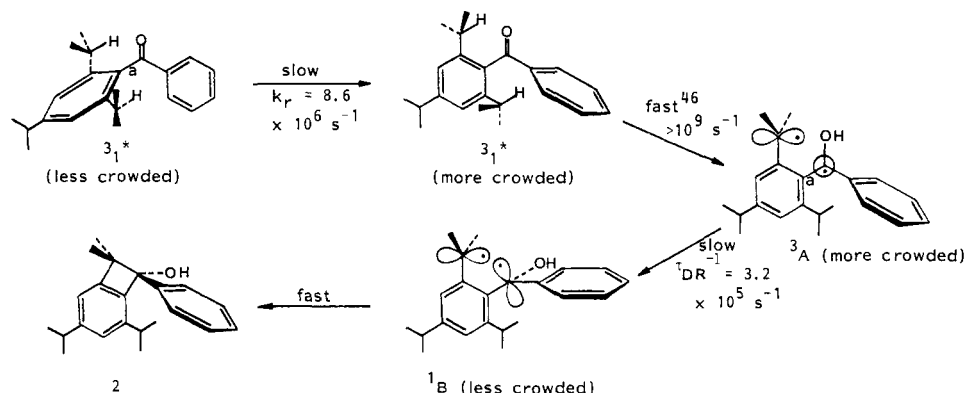
(36) The result contrasts with the postulate of Wirz^{18a} and Scaiano.³⁷ They interpreted their laser spectroscopic data for less hindered *o*-alkyl aromatic ketones with the assumption that the corresponding diradicals involve free syn-anti rotations.^{18a,37}

(37) Das, P. K.; Encina, M. V.; Small, R. D., Jr.; Scaiano, J. C. *J. Am. Chem. Soc.* 1979, 101, 6965.

(38) Since the product ratios may depend on the direction of approach to the intermediate (A or B), we are reluctant to quantitatively discuss the data in Scheme VII. But, if we assume that ¹B and ¹A are true intermediates in a sense that they are located at thermally equilibrated energy minima,³⁹ the data in Scheme VII indicate that



Scheme VIII



decay pathway of 3A is $^3A \rightarrow ^1B \rightarrow 2$ and that of 3B is $^3B \rightarrow ^1A \rightarrow 1$, both strongly following each adiabatic surface. In other words, the odd orbital rotation accompanying the rotation around bond a will create a favorable mode of vibration for mixing the singlet and triplet diradical states.

In the simplest terminology the ISC rate may be expressed by the golden rule in eq 7,⁴¹ where H_{SO} is a spin-orbit coupling

$$k_{ISC} = \frac{2\pi}{\hbar} \langle \psi_S | H_{SO} | \psi_T \rangle^2 F \rho \quad (7)$$

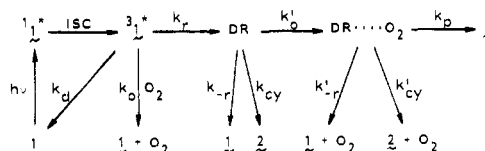
operator mixing singlet (ψ_S) and triplet (ψ_T) states, F is a Franck-Condon (vibrational) factor, and ρ is a state density factor. On the basis of a theoretical calculation of an electronic matrix element $\langle \psi_S | H_{SO} | \psi_T \rangle$, Salem proposed several rules for an effective S-T splitting of diradical states.⁴² Later general applicability of these rules were verified.¹¹

On the contrary, our experimental result (Scheme VII) should be relevant to the Franck-Condon factor F . Thus we propose that if a triplet surface intersects a singlet surface as a result of rotation of a lone-pair orbital in a certain diradical or diradicaloid molecule, an effective vibrational overlap (F) is created, leading to an efficient intersystem crossing, provided that the magnitude of the matrix element is substantial. Of course, nuclear motions on each surface tend to go to the energetically more feasible direction.

Experimental evidence which suggests the occurrence of such a coupled spin-flip and bond rotations is now rapidly accumulating for various other reactions. For example, the thermal decomposition of tetramethyl-1,2-dioxetane to produce a high yield of acetone triplet,^{43a} stereospecific triplet $[2+2]$ and $[4+2]$ cycloadditions,^{11c} magnetic-field-dependent CIDNP effects in type I cleavage of cyclohexanones,¹⁴ and substituent effects on the triplet lifetimes of a series of anisylalkenes^{43b} was interpreted in terms of ISC promoted by bond rotations.

A Factor Controlling the Lifetime of DR. The large P_p value (0.78, Scheme VI) indicates that the lifetime of DR generated from the direct photolysis of **1** (τ_{DR}) can be approximated by $1/k_{cy}$ ($\tau_{DR} = 1/(k_{cy} + k_{-r}) \sim 1/k_{cy}$). Therefore we here consider only the process $^3A \rightarrow ^1B \rightarrow 2$ as the factor determining τ_{DR} (Scheme VIII). Since, as we have shown in the preceding section, the diradical conformers 3A and 3B do not equilibrate during the lifetime of DR and since any singlet diradical in a favorable geometry (e.g., 1B) should readily collapse to the corresponding radical-coupling product^{13,40} (e.g., **2**), it is rational to say that τ_{DR} is determined by the rate of the sequence $^3A \rightarrow ^1B$. The control

Scheme IX



of τ_{DR} by the ISC rate was also revealed from the effect of para ring substituents on τ_{DR} .^{20b,44} Thus the rate constant for $^3A \rightarrow ^1B$ may be close to τ_{DR}^{-1} ($=3.2 \times 10^5 \text{ s}^{-1}$, Scheme VI) (Scheme VIII).

We have recently demonstrated that the intramolecular hydrogen-abstraction rate from the triplet state of **1** (k_r) is determined by the rate of sterically hindered rotation around bond a,¹⁵ i.e., the rate constant for the first step in Scheme VIII should be close to k_r ($=8.6 \times 10^6 \text{ s}^{-1}$, Scheme VI). One should note that this step proceeds faster than the sterically more favorable (more crowded \rightarrow less crowded) step $^3A \rightarrow ^1B$. It is probable that, although both steps involve rotations around the same bond (bond a), the rotation associated with the $^3A \rightarrow ^1B$ process is hampered by spin repulsion of the identical spin of the triplet diradical. In other words, 3A is really spin protected.

The Reactivity of $^1A^*$ and DR with Oxygen. The photolysis of **1** in the presence of oxygen afforded **2** and **4** (experiment 8 in Table I). The reaction mechanism is shown in Scheme IX, where $DR \cdots O_2$ is a complex analogous to that assumed in reactions between Norrish type II diradicals and ground-state oxygen.^{45b} Scheme IX gives eq 8, 9, and 10. We assume that, in analogy with the type II diradical-oxygen complex, the reketonization from $DR \cdots O_2$ is negligible ($k_{-r}' = 0$) and product formation from $DR \cdots O_2$ reflects a spin statistical factor ($k_{cy}'/k_p = 3$).^{45b} Since the values of Φ_T , τ_T , k_r , k_{cy} , and k_{-r} for **1** are already known (Scheme VI),^{15,20c} the rate constants for the reaction of oxygen with $^1A^*$ and DR (k_o and k_o' respectively) can be calculated straightforwardly according to eq 9 and 10, using the observed values of $\Phi(2)$ and $\Phi(4)$ (experiment 8 in Table I, $[O_2] = 1.91 \times 10^{-3} \text{ M}$).⁴⁷

$$\Phi(2) = \Phi_T \frac{k_r}{1/\tau_T + k_o[O_2]} \left(\frac{k_{cy}}{k_{cy} + k_{-r} + k_o'[O_2]} + \frac{k_o'[O_2]}{k_{cy} + k_{-r} + k_o'[O_2]} \frac{k_{cy}'}{k_{cy}' + k_{-r}' + k_p} \right) \quad (8)$$

$$\Phi(4) = \Phi_T \frac{k_r}{1/\tau_T + k_o[O_2]} \frac{k_o'[O_2]}{k_{cy} + k_{-r} + k_o'[O_2]} \frac{k_p}{k_{cy}' + k_{-r}' + k_p} \quad (9)$$

$$\frac{\Phi(2)}{\Phi(4)} = \frac{k_{cy}}{k_o'[O_2]} \frac{k_{cy}' + k_{-r}' + k_p}{k_p} + \frac{k_{cy}'}{k_p} \quad (10)$$

(39) (a) Michl, J. *Top. Curr. Chem.* **1974**, *46*, 1. (b) Michl, J. *Mol. Photochem.* **1972**, *4*, 243.

(40) Sevin, A.; Bigot, B.; Pfau, M. *Helv. Chim. Acta* **1979**, *62*, 699.

(41) Avouris, P.; Gelbart, W. M.; El-Sayed, M. A. *Chem. Rev.* **1977**, *77*, 793.

(42) The magnitude of S-T mixing depends on (a) the relative orientation of two odd orbitals, (b) the ionic character of the singlet state, and (c) the distance between two odd orbitals.^{10a}

(43) (a) Turro, N. J.; Lechtken, P. J. *Am. Chem. Soc.* **1973**, *95*, 264. (b) Caldwell, R. A.; Cao, C. V. *Ibid.* **1982**, *104*, 6174.

(44) The lifetimes of some type II and photoenolization diradicals are thought to be controlled by the ISC rate.^{13,45}

(45) (a) Small, R. D. Jr.; Scaiano, J. C. *J. Phys. Chem.* **1977**, *81*, 2126.

(b) Small, R. D., Jr.; Scaiano, J. C. *J. Am. Chem. Soc.* **1978**, *100*, 4512.

The results are that $k_0 = 1.9 \times 10^9 \text{ M}^{-1} \text{ s}^{-1}$ and $k_0' = 3.0 \times 10^7 \text{ M}^{-1} \text{ s}^{-1}$. It is noticeable that k_0' is much slower than the diffusion rate, while the same rate constant for other unhindered diradicals (triplet *o*-xylylenes and type II diradicals) is reported to be nearly diffusion controlled ($>10^9 \text{ M}^{-1} \text{ s}^{-1}$).^{18a-d,45b} However, the fact that the magnitude of k_0 is comparable to the rate for triplet quenching of various aromatic ketones^{45b,48} indicates that all our data are internally consistent.

It is commonly assumed that the diradical species that react readily with oxygen (triplet) are in their triplet states.^{7,18a-d,45b,49} Thus the rate constant k_0' may be regarded as that for the reaction between ^3A and O_2 .

The data of experiment 6 in Table I ($\Phi(4) = 0.031$) and of experiment 2 in Table III (0.1% yield of 4) suggest that ^3A is also formed from either the direct photochemical or thermal cleavage of 2.⁵⁰ It should be noted, however, that the product ratio 4/1 from the thermolysis (0.1/89 = 0.0011) is much smaller than that from the photolysis (0.031/0.20 = 0.16).

(46) (a) Wagner, P. J. *Pure Appl. Chem.* **1977**, *49*, 259. (b) Wagner, P. J.; Chen, C.-P. *J. Am. Chem. Soc.* **1976**, *98*, 239.

(47) Murov, S. L. "Handbook of Photochemistry"; Marcel Dekker: New York, 1973; pp 89.

(48) Garner, A.; Wilkinson, F. *Chem. Phys. Lett.* **1977**, *45*, 432.

(49) (a) Pagni, R. M.; Burnett, M. N.; Hassaneen, H. M. *Tetrahedron* **1982**, *38*, 843. (b) Wilson, R. M.; Wunderly, S. W.; Walsh, T. F.; Musser, A. K.; Outcalt, R.; Geiser, F.; Gee, S. K.; Brabender, W.; Yerino, L., Jr.; Conrad, T. T.; Tharp, G. A. *J. Am. Chem. Soc.* **1982**, *104*, 4429.

(50) The product ratio $\Phi(4)$ vs. $\Phi(2)$ obtained from the photooxidation of 2 (experiment 6 in Table I) is $\Phi(4)/\Phi(2) = 0.031/(1 - (0.20 + 0.031 + 0.01)) = 0.031/0.76 = 0.041$. This value is slightly smaller than that obtained from the photooxidation of 1 (experiment 8 in Table I, $\Phi(4)/\Phi(2) = 0.022/0.45 = 0.049$), although the oxygen concentration for the former reaction conditions ($[\text{O}_2] = 1.5 \times 10^{-2} \text{ M}$ in oxygen-saturated hexane⁴⁷) is about eight times that for the latter reaction conditions ($[\text{O}_2] = 1.9 \times 10^{-3} \text{ M}$ in air-saturated benzene⁴⁷). This fact also supports the idea that the diradical species photogenerated from 1 and 2 are kinetically distinguishable (^3A and ^1B , respectively).

There are several factors to be considered in order to explain this discrepancy, e.g., (1) the difference in oxygen concentrations,¹⁹ (2) effect of higher vibrational level reactions, and (3) the difference in Arrhenius activation parameters (E_a and $\log A$). A possible explanation in terms of the last point is as follows. From consideration of energy levels and spin multiplicities described in Figure 6, the ISC process $^1\text{B} \rightarrow ^3\text{A}$ may have smaller values for E_a and $\log A$ than the spin-allowed process $^1\text{B} \rightarrow ^1\text{A}$. As a result the path $2 \rightarrow ^1\text{B} \rightarrow ^1\text{A} \rightarrow 1$ can overwhelm the path $2 \rightarrow ^1\text{B} \rightarrow ^3\text{A} \rightarrow 4$ at the high temperatures required for thermolysis (134 °C). The same line of discussion was employed for competition between the triplet dimerization and the singlet ring closure of some trimethylenemethane diradicals.⁷

Experimental Section

Materials. 2,4,6-Triisopropylbenzophenone (1) and 4,6-diisopropyl-2,2-dimethyl-1-phenyl-1,2-dihydrobenzocyclobuten-1-ol (2) were prepared by a previous method.^{20e} Hexane, methanol, acetonitrile, acetone, and benzene were of spectral grade and used as received. Valerophenone and *tert*-butylbenzene were distilled before use.

The isolation and structural assignment of the anthrone 3 and the peroxide 4 have already been reported.^{20d,e}

The various instrumentations and the method for quantum yield measurements are the same as those described previously.¹⁵ However, 254-nm irradiations were performed with a 10-W low-pressure mercury lamp (Vycor lifter) and their quantum yields are based on ferrioxalate actinometry. All compounds, 1-4 and acetophenone, were analyzed with high-pressure liquid chromatography (silica gel column, hexane-ethyl acetate eluent) with use of methyl 2-naphthyl ketone as an internal standard.

Thermolyses were carried out on a 5-mL scale in a 10-mL two-necked flask.

Acknowledgment. We are indebted to the Ministry of Education of Japan for financial aid under a special research project.

Registry No. 1, 33574-11-7; 2, 33574-16-2; 3, 86177-63-1; 4, 86177-64-2; valerophenone, 1009-14-9; benzene, 71-43-2.

Looking at Chemistry as a Spin Ordering Problem

D. Maynau,* M. Said, and J. P. Malrieu

Contribution from the Laboratoire de Physique Quantique (ERA 821), Université Paul Sabatier, 31062 Toulouse Cedex, France. Received December 16, 1982

Abstract: The effective valence-bond Hamiltonian of Heisenberg type previously derived for the lowest states of π systems of conjugated molecules allows the projection of the information on neutral situations that differ only by spin ordering. The analysis of the wave function in terms of through-space spin correlation shows the dominance of spin alternation in the ground state and the spin wave nature of the lowest triplet. The strength of a bond is translated by the probability of finding a local singlet arrangement on it. This index (local singlet probability) nicely correlates with the experimental bond lengths. For free radicals (and triplet states) the projected wave function allows a direct estimate of spin densities.

The quasi-degenerate perturbation theory (QDPT)¹⁻⁷ is a fascinating tool that allows the building of effective Hamiltonians in a deductive way, in which the information is reduced to a low-dimensional problem. The "exact" or initial problem $H\Psi_m = E_m\Psi_m$ is transformed by considering a limited subspace $\{S\}$ of dimension n ; considering the projector P_S

$$P_S = \sum_{K \in S} |K\rangle\langle K|$$

one tries to find an effective Hamiltonian H^{eff} restricted to $\{S\}$ such that

$$\left. \begin{aligned} H^{\text{eff}}\psi_m &= E_m\psi_m \\ \psi_m &= P_S\Psi_m \end{aligned} \right\} m = 1, n$$

the n eigenvalues of H^{eff} are eigenvalues of H , and the eigenvectors ψ_m are projections of the corresponding n eigenvectors of H . The QDPT algorithms allow the fulfillment of this challenge in a perturbative way. Other iterative variational procedures are also available for the same purpose,⁸ derived from the Bloch equation.

- (1) J. H. Van Vleck, *Phys. Rev.*, **33**, 467 (1929).
- (2) J. des Cloiseaux, *Nucl. Phys.*, **20**, 321 (1960).
- (3) P. R. Certain and J. O. Hirschfelder, *J. Chem. Phys.*, **52**, 5977 (1970); **53**, 2992 (1970).
- (4) B. H. Brandow, *Rev. Mod. Phys.*, **39**, 771 (1967).
- (5) I. Shavitt and T. L. Redmon, *J. Chem. Phys.*, **73**, 5711 (1980).
- (6) G. Hose and U. Kaldor, *J. Phys. B*, **12**, 3827 (1979); *Phys. Scr.*, **21**, 357 (1980).
- (7) For a review of the chemical applications see B. H. Brandow, *4th Int. Symp. Quant. Chem.* (1982).

- (8) I. Lindgreen and J. Morrison, "Atomic Many Body Theory", Springer-Verlag, Berlin, 1982, p 381. Ph. Durand, *Phys. Rev.*, in press.